

See discussions, stats, and author profiles for this publication at: <https://www.researchgate.net/publication/6333892>

Construction of a Comb-Like Glycosylated Membrane Surface by a Combination of UV-Induced Graft Polymerization and Surface-Initiated ATRP

ARTICLE in LANGMUIR · JULY 2007

Impact Factor: 4.46 · DOI: 10.1021/la700275t · Source: PubMed

CITATIONS

68

READS

22

4 AUTHORS, INCLUDING:



Meng-Xin Hu

Zhejiang Gongshang University

19 PUBLICATIONS 672 CITATIONS

SEE PROFILE



Zhi-Kang Xu

Zhejiang University

251 PUBLICATIONS 6,277 CITATIONS

SEE PROFILE

Construction of a Comb-like Glycosylated Membrane Surface by a Combination of UV-Induced Graft Polymerization and Surface-Initiated ATRP

Qian Yang, Jing Tian, Meng-Xin Hu, and Zhi-Kang Xu*

Institute of Polymer Science, Key Laboratory of Macromolecular Synthesis and Functionalization (Ministry of Education), and State Key Laboratory of Chemical Engineering, Zhejiang University, Hangzhou 310027, PR China

Received January 31, 2007. In Final Form: March 16, 2007

Carbohydrate residues are found on the extracellular side of the cell membrane. They form a protective coating on the outer surface of the cell and are involved in intercellular recognition. Synthetic carbohydrate-based polymers, so-called glycopolymers, are emerging as important well-defined tools for investigating carbohydrate-based biological processes and for simulating various functions of carbohydrates. In this work, the surface of a polypropylene microporous membrane (PPMM) was modified with comb-like glycopolymers by a combination of UV-induced graft polymerization and surface-initiated atom-transfer radical polymerization (ATRP). 2-Hydroxyethyl methacrylate (HEMA) was first grafted to the PPMM surface under UV irradiation in the presence of benzophenone and ferric chloride. ATRP initiator was then coupled to the hydroxyl groups of poly(HEMA) brushes. Surface-initiated ATRP of a glycomonomer, D-gluconamidoethyl methacrylate, was followed at ambient temperature in aqueous solvent. Water had a significant acceleration effect on the ATRP process; however, loss of control over the polymerization process was also observed. The addition of CuBr₂ to the ATRP system largely increased the controllability at the cost of the polymerization rate. The grafting of HEMA, the coupling of ATRP initiator to the hydroxyl groups, and the surface-initiated ATRP were confirmed by Fourier transform infrared spectroscopy and X-ray photoelectron spectroscopy.

Introduction

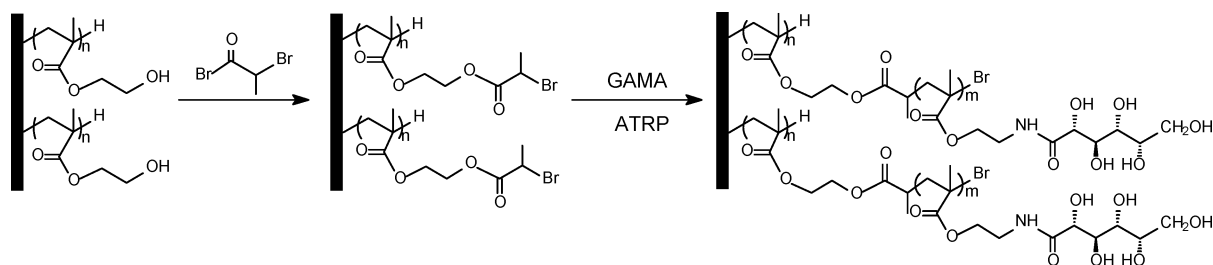
Tethering of polymer brushes covalently onto a solid substrate by surface-initiated polymerization is a versatile and effective method of altering the surface properties of the material.¹ The grafted polymer chains are crowded and stretch away from the surface, serving as a secondary boundary between the material and the environment.² It has been found subsequently that polymer brushes are very useful in many fields such as protein-resistant surfaces,³ enzyme immobilization,⁴ and stimulation-responsive surfaces.⁵ Various techniques, such as UV irradiation,⁶ plasma treatment,⁷ an ozone method⁸ and γ -ray irradiation,⁹ have been

widely applied in the surface modification of diverse materials. However, these conventional methods suffer from the disadvantages of lacking control over the chain structure (molecular weight, polydispersity, and terminal chain functionality) of the grafted polymers. With the progress in polymerization methods, it is possible to prepare well-defined polymer brushes on various substrates by cationic polymerization,¹⁰ anionic polymerization,¹¹ ring-opening metathesis polymerization (ROMP),¹² nitroxide-mediated polymerization (NMP),¹³ reversible addition–fragmentation chain-transfer polymerization (RAFT),¹⁴ and atom-transfer radical polymerization (ATRP)¹⁵ in a living/controlled manner. Among these living/controlled approaches, ATRP is especially attractive and garners much more attention because

* To whom all correspondence should be addressed. E-mail: xuzk@zju.edu.cn. Fax: ++ 86 571 8795 1773.

- (1) Bhattacharya, A.; Misra, B. N. *Prog. Polym. Sci.* **2004**, *29*, 767.
- (2) Zhao, B.; Brittain, W. J. *Prog. Polym. Sci.* **2000**, *25*, 677.
- (3) (a) Stine, R.; Pishko, M. V.; Hampton, J. R.; Dameron, A. A.; Weiss, P. S. *Langmuir* **2005**, *21*, 11352. (b) Ma, H. W.; Li, D. J.; Sheng, X.; Zhao, B.; Chilkoti, A. *Langmuir* **2006**, *22*, 3751. (c) Chang, Y.; Chen, S. F.; Zhang, Z.; Jiang, S. Y. *Langmuir* **2006**, *22*, 2222. (d) Wazawa, T.; Ishizuka-Katsura, Y.; Nishikawa, S.; Iwane, A. H.; Aoyama, S. *Anal. Chem.* **2006**, *78*, 2549.
- (4) (a) Deng, H. T.; Xu, Z. K.; Huang, X. J.; Wu, J.; Seta, P. *Langmuir* **2004**, *20*, 10168. (b) Deng, H. T.; Xu, Z. K.; Dai, Z. W.; Wu, J.; Seta, P. *Enzyme Microb. Technol.* **2005**, *36*, 996. (c) Deng, H. T.; Xu, Z. K.; Liu, Z. M.; Wu, J.; Ye, P. *Enzyme Microb. Technol.* **2004**, *35*, 437. (d) Liu, Z. M.; Tingry, S.; Innocent, C.; Durand, J.; Xu, Z. K.; Seta, P. *Enzyme Microb. Technol.* **2006**, *39*, 868.
- (5) (a) Ito, Y.; Ochiai, Y.; Park, Y. S.; Imanishi, Y. *J. Am. Chem. Soc.* **1997**, *119*, 1619. (b) Kidoaki, S.; Ohya, S.; Nakayama, Y.; Matsuda, T. *Langmuir* **2001**, *17*, 2402. (c) Volpe, C. D.; Cassinelli, C.; Morra, M. *Langmuir* **1998**, *14*, 4650. (d) Liang, L.; Shi, M.; Viswanathan, V. V.; Peurung, L. M.; Young, J. S. *J. Membr. Sci.* **2000**, *177*, 97.
- (6) (a) Thom, V. H.; Altankov, G.; Groth, Th.; Jankova, K.; Jonsson, G.; Ulbricht, M. *Langmuir* **2000**, *16*, 2756. (b) Ulbricht, M.; Yang, H. *Chem. Mater.* **2005**, *17*, 2622. (c) Ma, H.; Davis, R. H.; Bowman, C. N. *Macromolecules* **2000**, *33*, 331.
- (7) (a) Wavhal, D. S.; Fisher, E. R. *Langmuir* **2003**, *19*, 79. (b) Kou, R.-Q.; Xu, Z.-K.; Deng, H.-T.; Liu, Z.-M.; Seta, P.; Xu, Y.-Y. *Langmuir* **2003**, *19*, 6869. (c) Teare, D. O. H.; Schofield, W. C. E.; Roucoules, V.; Badyal, J. P. S. *Langmuir* **2003**, *19*, 2398.
- (8) (a) Wang, Y.; Kim, J. H.; Choo, K. H.; Lee, Y. S.; Lee, C. H. *J. Membr. Sci.* **2000**, *169*, 269. (b) Park, H. B.; Han, D. W.; Lee, Y. M. *Chem. Mater.* **2003**, *15*, 2346. (c) Ostenson, M.; Gatenholm, P. *Langmuir* **2005**, *21*, 160.

- (9) (a) Shim, J. K.; Na, H. S.; Lee, Y. M.; Huh, H.; Nho, Y. C. *J. Membr. Sci.* **2001**, *190*, 215. (b) Yang, J. M.; Lin, H. T. *J. Membr. Sci.* **2004**, *243*, 1. (c) Tanaka, H.; Sato, N.; Matsuyama, T. *Langmuir* **2005**, *21*, 7696.
- (10) (a) Jordan, R.; West, N.; Ulman, A.; Chou, Y. M.; Nuyken, O. *Macromolecules* **2001**, *34*, 1606. (b) Jordan, R.; Ulman, A. *J. Am. Chem. Soc.* **1998**, *120*, 243.
- (11) (a) Advincula, R.; Zhou, Q. G.; Park, M.; Wang, S. G.; Mays, J.; Sakellariou, G.; Pispas, S.; Hadjichristidis, N. *Langmuir* **2002**, *18*, 8672. (b) Fan, X. W.; Zhou, Q. Y.; Xia, C. J.; Cristofoli, W.; Mays, J.; Advincula, R. *Langmuir* **2002**, *18*, 4511. (c) Zhou, Q. Y.; Wang, S. X.; Fan, X. W.; Advincula, R.; Mays, J. *Langmuir* **2002**, *18*, 3324.
- (12) (a) Harada, Y.; Girolami, G. S.; Nuzzo, R. G. *Langmuir* **2003**, *19*, 5104. (b) Kim, N. Y.; Jeon, N. L.; Choi, I. S.; Takami, S.; Harada, Y.; Finnie, K. R.; Girolami, G. S.; Nuzzo, R. G.; Whitesides, G. M.; Laibinis, P. E. *Macromolecules* **2000**, *33*, 2793. (c) Yoon, K. R.; Koh, Y. J.; Choi, I. S. *Macromol. Rapid Commun.* **2003**, *24*, 207.
- (13) (a) Andruzzi, L.; Hexemer, A.; Li, X. F.; Ober, C. K.; Kramer, E. J.; Galli, G.; Chiellini, E.; Fischer, D. A. *Langmuir* **2004**, *20*, 10498. (b) Li, J.; Chen, X. R.; Chang, Y. C. *Langmuir* **2005**, *21*, 9562.
- (14) (a) Hong, C. Y.; You, Y. Z.; Pant, C. Y. *Chem. Mater.* **2005**, *17*, 2247. (b) Ying, L.; Yu, W. H.; Kang, E. T.; Neoh, K. G. *Langmuir* **2004**, *20*, 6032. (c) Yu, W. H.; Kang, E. T.; Neoh, K. G. *Langmuir* **2005**, *21*, 450. (d) Baum, M.; Brittain, W. J. *Macromolecules* **2002**, *35*, 610. (e) Yoshikawa, C.; Goto, A.; Tsujii, Y.; Fukuda, T.; Yamamoto, K.; Kishida, A. *Macromolecules* **2005**, *38*, 4604. (f) Barner, L.; Zwaneveld, N.; Perera, S.; Pham, Y.; Davis, T. P. *J. Polym. Sci., Polym. Chem.* **2002**, *40*, 4180. (g) Chen, Y. W.; Sun, W.; Deng, Q. L.; Chen, L. J. *Polym. Sci., Part A: Polym. Chem.* **2006**, *44*, 3071. (h) Xu, G. Y.; Wu, W. T.; Wang, Y. S.; Pang, W. M.; Zhu, Q. R.; Wang, P. H.; You, Y. Z. *Polymer* **2006**, *47*, 5909.

Scheme 1. Schematic Representation for the Coupling of 2-Bromopropionyl Bromide to the PHEMA Brushes and Surface-Initiated ATRP of GAMA

of its tolerance for impurities and mild polymerization conditions compared with the conditions for ionic polymerization and ROMP. Also, this controlled radical polymerization is compatible with a wide range of monomers such as styrene, acrylates, and methacrylates. With its living character, the ATRP process yields polymers with a low polydispersity and permits the synthesis of block copolymers by the activation of dormant chain ends.¹⁶ In addition, polymers with comb, hyperbranched, or star architecture can also be obtained by ATRP processes.

Glycobiology, a newly developed subject that deals with the nature and role of carbohydrates in biological events, has attracted much interest recently. Carbohydrates have been found on the surface of nearly every cell (glycocalyx) in the form of polysaccharides, glycoproteins, glycolipids, and other glycoconjugates and has been proven to play essential roles in many biological processes. They serve as recognition sites for docking other cells, molecules, and pathogens or as factors controlling the generation of biological functions.¹⁷ However, they also contribute to the steric repulsion that prevents the undesirable nonspecific adhesion of other proteins and cells.¹⁸ These two aspects rely on carbohydrate–protein interactions whereas the mechanisms remain controversial even today. Indeed, though the mechanism is not very well known, it is clear that the carbohydrate–protein interactions rely on the aggregation of the ligands both for the prevention of undesirable nonspecific adhesion and for specific recognition. Actually, highly aggregated surface-tethered carbohydrate ligands, like the glycocalyx on the cell surface, result in not only the enhancement of binding strength in specific recognition against proteins¹⁹ but also the minimization of nonspecific protein adsorption.¹⁸ Mimicry of the cell surface glycocalyx has led to many promising applications, and a large number of different synthetic multivalent glycoligands (such as glycoclusters, glycodendrimers, glycopolymers, etc.) have been designed to interfere effectively with carbohydrate–protein interactions. Synthetic carbohydrate-based polymers—glycopolymers—are emerging as an important well-defined tool

for investigating carbohydrate–protein interactions²⁰ because of advantages such as very high valency, the ease of controlling the molecular structure, and the ability to vary the species of the sugar ligands. In the past decade, a great number of sugar-containing monomers and their polymers have been synthesized as reviewed by Wang et al.,²¹ Ladmiral et al.,²² and Okada et al.²³ In our previous work, glycopolymers were grafted onto polymer membranes to give glycocalyx-like layer tethered surfaces.²⁴ However, conventional graft techniques suffer from a lack of control over chain structures and molecular weight as mentioned above. Surface-tethered glycopolymers with different chain structures and chain lengths may show diverse interaction kinetics with proteins. However, it is also suggested that the random clustering of carbohydrates sometimes reduces the strength of affinity with guest proteins owing to the sterically hindered sugar branches.²⁵ In other words, the glycopolymer chain length may greatly affect the recognition activity.²⁶ As a consequence, the generation of glycopolymers with well-defined chain structure and appropriate sugar density becomes largely demanded. Some efforts have been undertaken for this purpose by ATRP²⁷ and RAFT-mediated²⁸ polymerization. In this work, we describe a method to tether a comb-like glycopolymer with controllable chain structure on the surface of a polypropylene microporous membrane (PPMM) by a combination of UV-induced graft polymerization and surface-initiated ATRP. 2-Hydroxyethyl methacrylate (HEMA) was first grafted onto the PPMM surface by UV-induced graft polymerization. The reaction between the hydroxyl group and 2-bromopropionyl bromide gave the immobilization of the ATRP initiator. Then, the surface-initiated ATRP of a sugar-containing monomer was carried out and resulted in well-defined comb-like glycopolymer brushes. By taking advantage of ATRP, one can control the chain length of the glycopolymer; subsequently, this control of chain length is expected to modulate the interactions with proteins.

- (15) (a) Li, L.; Lukehart, C. M. *Chem. Mater.* **2006**, *18*, 94. (b) Tanke, R. S.; Kaulzarich, S. M.; Patten, T. E.; Pettigrew, K. A.; Murphy, D. L.; Thompson, M. E.; Lee, H. W. *H. Chem. Mater.* **2003**, *15*, 1682. (c) Xu, F. J.; Kang, E. T.; Neoh, K. G. *Macromolecules* **2005**, *38*, 1573. (d) Xu, F. J.; Song, Y.; Cheng, Z. P.; Zhu, X. L.; Zhu, C. X.; Kang, E. T.; Neoh, K. G. *Macromolecules* **2005**, *38*, 6254. (e) Liu, Y.; Klep, V.; Zdyrko, B.; Luzinov, I. *Langmuir* **2004**, *20*, 6710. (f) Li, D. J.; Jones, G. L.; Dunlap, J. R.; Hua, F. J.; Zhao, B. *Langmuir* **2006**, *22*, 3344. (g) Xu, F. J.; Cai, Q. J.; Kang, E. T.; Neoh, K. G. *Langmuir* **2005**, *21*, 3221. (h) Yu, W. H.; Kang, E. T.; Neoh, K. G. *Langmuir* **2004**, *20*, 8294. (i) Ma, H. W.; Li, D. J.; Sheng, X.; Zhao, B.; Chilkoti, A. *Langmuir* **2006**, *22*, 3751. (j) Save, M.; Granvorka, G.; Bernard, J.; Charleux, B.; Boissiere, C.; Grosso, D.; Sanchez, C. *Macromol. Rapid Commun.* **2006**, *27*, 393. (k) Feng, W.; Chen, R. X.; Brash, J. L.; Zhu, S. P. *Macromol. Rapid Commun.* **2005**, *26*, 1383. (l) Ramakrishnan, A.; Dhamodharan, R.; Ruhe, J. *Macromol. Rapid Commun.* **2002**, *23*, 612. (16) Edmondson, S.; Osborne, V. L.; Huck, W. T. S. *Chem. Soc. Rev.* **2004**, *33*, 14. (17) Dwek, R. A. *Chem. Rev.* **1996**, *96*, 683. (18) Holland, N. B.; Qiu, Y.; Ruegsegger, M.; Marchant, R. E. *Nature* **1998**, *392*, 799. (19) Lee, Y. C.; Lee, R. T. *Acc. Chem. Res.* **1995**, *28*, 321.

- (20) Lis, H.; Sharon, N. *Chem. Rev.* **1998**, *98*, 637. (21) Wang, Q.; Dordick, J. S.; Linhardt, R. J. *Chem. Mater.* **2002**, *14*, 3232. (22) Ladmiral, V.; Melia, E.; Haddleton, D. M. *Eur. Polym. J.* **2004**, *40*, 431. (23) Okada, M. *Prog. Polym. Sci.* **2001**, *26*, 67. (24) (a) Yang, Q.; Xu, Z. K.; Dai, Z. W.; Wang, J. L.; Ulbricht, M. *Chem. Mater.* **2005**, *17*, 3050. (b) Yang, Q.; Xu, Z. K.; Hu, M. X.; Li, J. J.; Wu, J. *Langmuir* **2005**, *21*, 10717. (c) Yang, Q.; Hu, M. X.; Dai, Z. W.; Tian, J.; Xu, Z. K. *Langmuir* **2006**, *22*, 9345. (25) Furuie, T.; Nishi, N.; Tokura, S.; Nishimura, S. *Macromolecules* **1995**, *28*, 7241. (26) Mann, D. A.; Kanai, M.; Maly, D. J.; Kiessling, L. L. *J. Am. Chem. Soc.* **1998**, *120*, 10575. (27) (a) Ejaz, M.; Ohno, K.; Tsujii, Y.; Fukuda, T. *Macromolecules* **2000**, *33*, 2870. (b) Muthukrishnan, S.; Zhang, M. F.; Burkhardt, M.; Drechsler, M.; Mori, H.; Muller, A. H. E. *Macromolecules* **2005**, *38*, 7926. (c) Muthukrishnan, S.; Plamper, F.; Mori, H.; Muller, A. H. E. *Macromolecules* **2005**, *38*, 10631. (28) (a) Stenzel, M. H.; Zhang, L.; Huck, W. T. S. *Macromol. Rapid Commun.* **2006**, *27*, 1121. (b) Spain, S. G.; Albertin, L.; Cameron, N. R. *Chem. Commun.* **2006**, 4198. (c) Albertin, L.; Stenzel, M.; Barner-Kowollik, C.; Foster, L. J. R.; Davis, T. P. *Macromolecules* **2004**, *37*, 7530. (d) Albertin, L.; Stenzel, M. H.; Barner-Kowollik, C.; Foster, L. J. R.; Davis, T. P. *Macromolecules* **2005**, *38*, 9075.

Experimental Section

Materials. PPMM, prepared by the thermally induced phase separation (TIPS) method, with an average pore size of 0.20 μm and a relatively high porosity of about 80% was purchased from Membrana GmbH (Germany). All of the membrane samples used in this study were cut into rounds with a diameter of 3.95 cm (area = 12.25 cm^2). Before surface modification, the membrane was washed with acetone for 0.5 h to remove any impurity adsorbed onto the surface, dried in a vacuum oven in 40 $^\circ\text{C}$ to constant weight (W_0), and then stored in desiccator. D-Gluconamidoethyl methacrylate (GAMA) was synthesized in our laboratory as described previously.^{24a} Triethylamine (TEA) was purified by distillation and stored in 4 Å molecular sieves. Tetrahydrofuran (THF) was washed with stannous chloride solution, refluxed with sodium using benzophenone as an indicator, and distilled before use. HEMA (98%, Aldrich) and 2-bromopropionyl bromide (97%, Fluka) were used as received. CuBr was purified according to the reported procedures.²⁹ CuBr₂ (99.9%) was a commercial product and was used without further purification. 2,2'-Bipyridine (Bpy), FeCl₃·6H₂O, benzophenone, acetone, and methanol were analytical grade and were used without further purification. Water used in all syntheses and measurements was deionized and ultrafiltrated to 18 M Ω .

UV-Induced Graft Polymerization of HEMA. HEMA was grafted onto the PPMM surface by UV-induced graft polymerization in the presence of benzophenone and FeCl₃·6H₂O as described in our previous work.³⁰ Briefly, benzophenone, FeCl₃·6H₂O, and HEMA were dissolved in acetone/water (1/1). Thereafter, a sample of PPMM was dipped in the solution for 60 min and then put into a UV processor, which was equipped with two 300 W high-pressure mercury lamps. After 10 min of purging with nitrogen gas, UV irradiation was carried out for 20 min under a nitrogen gas environment. Finally, the modified membrane was washed with acetone for 4 h and then with pure water for 20 h by vibration to remove any homopolymer and adsorbed monomer. After being dried in a vacuum oven at 40 $^\circ\text{C}$ to constant weight, the membrane was weighed (W_1) with an analytical balance to a precision of 0.1 mg. The amount (mol) of grafted HEMA was calculated from

$$N_{\text{HEMA}} = \frac{W_1 - W_0}{130}$$

where 130 is the repeat unit mass of the grafted poly(HEMA) chain.

Immobilization of the ATRP Initiator. Immobilization of the ATRP initiator on the poly(HEMA) (PHEMA)-functionalized PPMM surface (PPMM-g-PHEMA) was achieved by the reaction between 2-bromopropionyl bromide and the hydroxyl group (PPMM-g-PHEMA-Br). Three pieces of the PHEMA-functionalized PPMMs were immersed in 60 mL of anhydrous THF at 0 $^\circ\text{C}$, and 3.96 mL (0.0285 mol) of dry TEA was added. Then 3 mL (0.0285 mol) of 2-bromopropionyl bromide dissolved in 40 mL of anhydrous THF was added dropwise under a nitrogen atmosphere. The mixture was stirred for another 3 h at 0 $^\circ\text{C}$, followed by stirring at room temperature for 24 h. After the reaction, PPMMs were thoroughly washed with methanol–water–methanol in sequence and dried under vacuum at 40 $^\circ\text{C}$ to constant weight (W_2).

ATRP on the PPMM-g-PHEMA-Br Surface. The PPMM-g-PHEMA-Br substrate, CuBr (0.018 g, 0.13 mmol), and Bpy (0.04 g, 0.26 mmol) were added to a 50 mL Schlenk flask, and then the flask was sealed. The flask was evacuated and back-filled with nitrogen three times. GAMA (4 g, 13 mmol) was dissolved in methanol/water (30 mL) and purged with nitrogen for 30 min. Afterwards, the monomer solution was transferred into the flask via cannula, and the reaction mixture was shaken at 30 $^\circ\text{C}$ for predetermined time. In a typical surface-initiated ATRP run with CuBr₂, the same procedure was adopted except that 0.0058 g (0.026 mmol) of CuBr₂ was added to the reaction system. After the reaction,

polymerization was terminated by exposure to air, and then the PPMM with glycopolymer brushes was removed from the reaction mixture. After being thoroughly washed with methanol and water, the membrane was dried to constant weight (W_3) under vacuum at 40 $^\circ\text{C}$.

Calculation of the Degree of Polymerization. The degree of polymerization (DP) was calculated from mass weighting data and X-ray photoelectron spectroscopy (XPS) data (Supporting Information). The XPS method was used as a contrast, and all calculations were based on data obtained by the mass weighting method as follows: the amount (mol) of immobilized ATRP initiator (–Br) was

$$N_{\text{Br}} = \frac{W_2 - W_1}{135}$$

and the amount of GAMA grafted by surface-initiated ATRP was

$$N_{\text{GAMA}} = \frac{W_3 - W_2}{307}$$

Thus, the degree of polymerization could be defined as

$$\text{PD} = \frac{N_{\text{GAMA}}}{N_{\text{Br}}}$$

where 135 is the molecular weight increase gained by the immobilization of the ATRP initiator. The repeat unit mass of grafted poly(GAMA) chains is 307. Here, for the convenience of calculation, we assumed that the grafting chains grew from every initiator symmetrically, and we ignored the weight decrease caused by the loss of the terminal Br.

Surface Characterization. To investigate the variation in surface chemical structure and morphology before and after HEMA grafting and ATRP initiator immobilization and to confirm the surface-initiated ATRP of GAMA, several surface characterization techniques were used (attenuated total reflectance Fourier transform infrared spectroscopy (FTIR/ATR) and XPS).

FTIR/ATR measurements were carried out on a Vector 22 FTIR (Bruker Optics, Switzerland) equipped with an ATR cell (KRS-5 crystal, 45 $^\circ$). Sixteen scans were taken for each spectrum at a resolution of 4 cm^{-1} . XPS measurements of the original and modified membranes were performed on a PHI-5000C ESCA system (Perkin-Elmer) with Al K α radiation ($h\nu = 1486.6 \text{ eV}$). In general, the X-ray anode was run at 250 W, and the high voltage was kept at 14.0 kV with a detection angle of 45 $^\circ$. The pass energy was fixed at 93.9 eV to ensure sufficient sensitivity. The base pressure of the analyzer chamber was about 5×10^{-7} Pa. The survey spectra (from 0 to $\sim 1200 \text{ eV}$) and the core-level spectra with much high resolution were both recorded. Binding energies were calibrated using containment carbon (C 1s = 284.7 eV). The data analysis was carried out on the PHI-MATLAB software provided by PHI Corporation. No radiation damage was observed during the data collection time.

Results and Discussion

Preparation of PPMM-g-PHEMA and Immobilization of the ATRP Initiator. PPMM was first functionalized with PHEMA by UV-induced graft polymerization. An important feature of PHEMA is that the hydroxyl groups can serve as reactive sites for the coupling of various functional groups with a nearly quantitative conversion of hydroxyl groups.³¹ The graft polymerization was carried out in the presence of FeCl₃, without which no grafting was observed.³⁰ FTIR/ATR spectra for nascent PPMM and PPMM-g-PHEMA are shown in Figure 1a,b, respectively. It can be seen that the PHEMA-functionalized PPMM surface shows a characteristic peak at 1725 cm^{-1} due to C=O stretching in the carbonyl group. An additional broad

(29) Matyjaszewski, K.; Miller, P. J.; Shukla, N.; Immaraporn, B.; Gelman, A.; Luokala, B. B.; Siclován, T. M.; Kickelbick, G.; Vallant, T.; Hoffmann, H.; Pakula, T. *Macromolecules* **1999**, 32, 8716.

(30) Hu, M. X.; Yang, Q.; Xu, Z. K. *J. Membr. Sci.* **2006**, 285, 195.

(31) Huang, W. X.; Kim, J. B.; Bruening, M. L.; Baker, G. L. *Macromolecules* **2002**, 35, 1175.

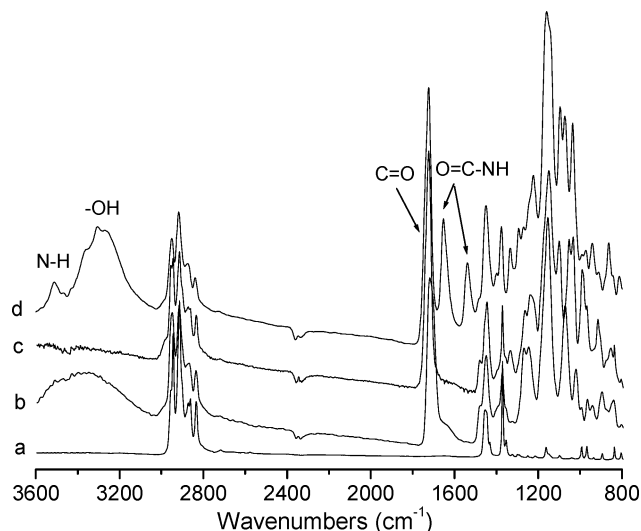


Figure 1. IR spectra of nascent PPMM (a), PPMM-g-PHEMA (b), PPMM-g-PHEMA-Br (c), and PPMM-g-PHEMA-co-GAMA (d; ATRP conditions, [GAMA]/[CuBr]/[CuBr₂]/[Bpy] = 100/1/0.25/2; solvent, methanol/water = 4/1; polymerization time, 6 h).

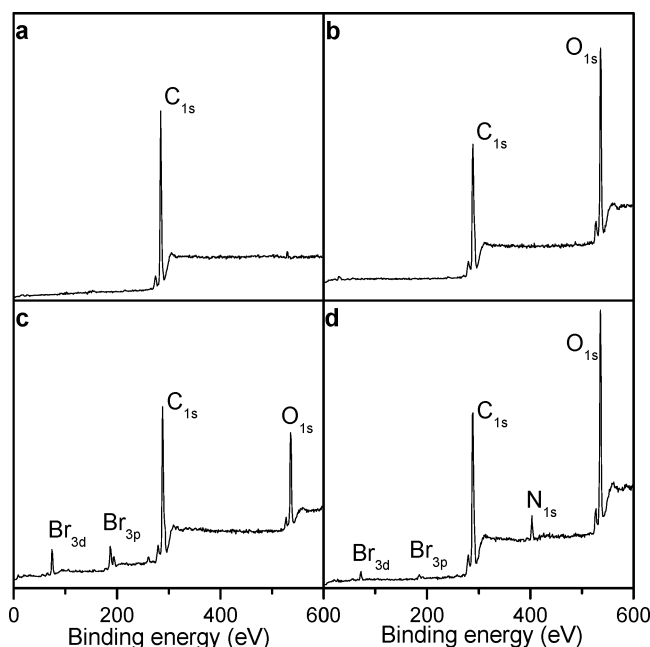


Figure 2. XPS spectra of nascent PPMM (a), PPMM-g-PHEMA (b), PPMM-g-PHEMA-Br (c), and PPMM-g-PHEMA-co-GAMA (d; ATRP conditions, [GAMA]/[CuBr]/[Bpy] = 100/1/2; solvent, methanol/water = 4/1; polymerization time, 6 h).

absorption band at about 3000–3600 cm⁻¹, assigned to the —OH stretching vibration, was also found for PPMM-g-PHEMA. The graft polymerization of HEMA was also ascertained by XPS analysis. For the nascent PPMM surface, only one major emission peak at 284.7 eV ascribed to the binding energy of C 1s was found (Figure 2a). However, an additional peak at 534.0 eV, corresponding to the binding energy of O 1s, was detected from the spectrum of the PPMM-g-PHEMA surface. In addition, the C 1s core-level spectrum of the PPMM-g-PHEMA surface could be resolved into three peaks (Figure 3a). One of them at the binding energy of 284.7 eV was assigned to C—H and C—C. Another two peaks at binding energies of 286.2 and 288.4 eV were ascribed to the C atoms bonded to the hydroxyl group (C—O) and the ester group (O=C—O).

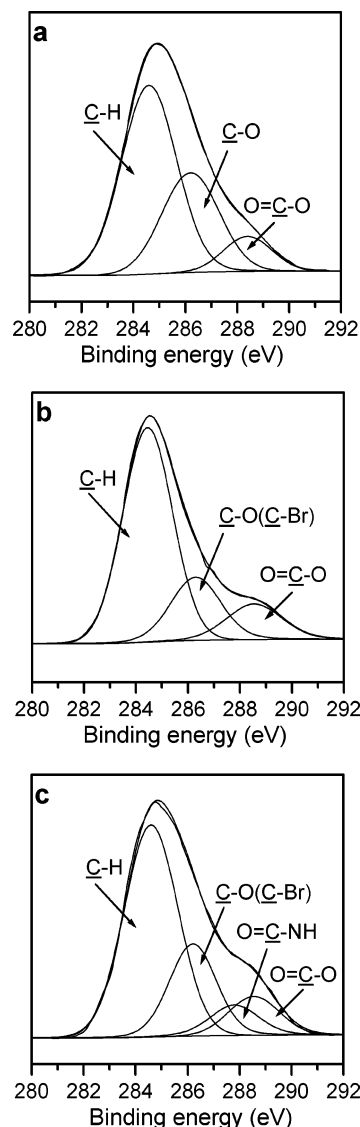


Figure 3. C 1s core-level spectra of PPMM-g-PHEMA (a), PPMM-g-PHEMA-Br (b), and PPMM-g-PHEMA-co-GAMA (c; ATRP conditions, [GAMA]/[CuBr]/[Bpy] = 100/1/2; solvent, methanol/water = 4/1; polymerization time, 6 h).

Matyjaszewski et al.³² and Sawamoto et al.³³ reported that organic halides with a potentially active carbon—halogen bond, especially α -bromoester, could be widely used as an initiator for ATRP of various monomers including styrene, acrylates, methacrylate, and some other vinyl monomers. For the immobilization of the ATRP initiator, the hydroxyl groups on the tethered PHEMA chains were reacted with 2-bromopropionyl bromide. This reaction was carried out in dry THF under the protection of N₂ because 2-bromopropionyl bromide was moisture-sensitive and highly corrosive. The reaction time was prolonged to 24 h at room temperature to expect complete reaction for the hydroxyl groups on the tethered PHEMA chains. However, as shown in Table 1, a bromination ratio of only about 62% was obtained. This might be ascribed to the increased steric hindrance of the hydroxyl groups near the substrate surface. Also, the reaction between hydroxyl groups and 2-bromopropionyl bromide took place preferably at the outer part. The initiator immobilization was confirmed by the appearance of Br 3d (70.5 eV) and Br 3p (187.7 eV) peaks in the XPS spectrum (Figure 2c). Moreover,

(32) Matyjaszewski, K.; Xia, J. H. *Chem. Rev.* **2001**, *101*, 2921.

(33) Kamigaito, M.; Ando, T.; Sawamoto, M. *Chem. Rev.* **2001**, *101*, 3689.

Table 1. Typical Results for Chemical Composition and Bromination Ratio of the Functionalized PPMM Surfaces

samples	chemical composition			bromination ratio (%)	
	[C–O(C–Br)]/[O=C–O] ^a	[C]/[O] ^b	[O]/[Br] ^c	<i>R</i> _{weight} ^d	<i>R</i> _{XPS} ^e
PPMM-g-HEMA	2.15/1.00 (2.00/1.00)	2.23/1.00 (2.00/1.00)	0	62.10	60.98
PPMM-g-HEMA-Br	1.61/1.00 (1.50/1)	2.51/1.00 (2.25/1.00)	5.92/1.00 (4.00/1)		

^a Determined from the XPS curve-fitted C 1s core-level spectra. Values in parentheses are the theoretical ratios for PHEMA and PHEMA-Br, respectively. ^b Determined from the sensitivity-factor-corrected C 1s and O 1s core-level spectral area ratio. Values in parentheses are the theoretical ratios of PHEMA and PHEMA-Br (100% bromination ratio), respectively. ^c Determined from the sensitivity-factor-corrected O 1s and Br 3d core-level spectral area ratio. The value in parentheses is the theoretical ratio of PHEMA-Br (100% bromination ratio). ^d Value calculated from mass weighting results as $R_{\text{weight}} = N_{\text{Br}}/N_{\text{HEMA}}$, in which $N_{\text{Br}} = 21.50 \mu\text{mol}$ and $N_{\text{HEMA}} = 34.62 \mu\text{mol}$. ^e Value calculated from core-level spectral area ratio of Br 3d and O 1s as $R_{\text{XPS}} = 3/([O]/[Br]-1)$.

Table 2. ATRP of GAMA from the PPMM-g-HEMA-Br Surface under Various Experimental Conditions

samples ^a	solvents (v/v) methanol/H ₂ O	GAMA/Bpy/CuBr/CuBr ₂ (molar ratio)	ATRP time (h)	degree of polymerization	
				I ^b	II ^c
GAMA-g-HEMA-co-GAMA	3/2	100/2/1/0	1	11	14
			5	12	15
	4/1	100/2/1/0	1	6	7
			5	18	21
		100/2/1/0.25	2	12	18
			5	20	26
		100/2/1/0.5	2	5	4
			4	10	13

^a All polymerizations were carried out at 30 °C. ^b Values calculated from mass weighting results as described in the Experimental Section. ^c Values calculated by the method described in Supporting Information.

in the FTIR/ATR spectra, the complete disappearance of the –OH peak (3000–3600 cm^{−1}) indicated a nearly quantitative conversion of the hydroxyl groups to corresponding esters, which was consistent with the increase of the C=O peak at 1725 cm^{−1} (Figure 1c).

Fabrication of Comb-like Glycopolymer Brushes on PPMM-g-PHEMA-Br by Surface-Initiated ATRP. Narain et al.³⁴ first reported the synthesis and ATRP of GAMA. The polymerization process was well controlled, and glycopolymers with relatively low polydispersities were obtained in their work. In this work, with the attached 2-bromopropionyl groups, the tethered PHEMA chains was used as a surface macroinitiator for the subsequent surface-initiated ATRP of GAMA to form comb-like glycopolymer brushes. This process was expected to control the sequence length of the glycopolymer and to enhance the packing density of the sugar residues substantially. We used a methanol/water solution system for the ATRP of GAMA. Water increased the dissolvability of the catalysts and kept the reaction system inhomogeneous. However, Matyjaszewski et al.³⁵ showed that polar solvents resulted in an increase in the activation rate constant as well as a decrease in the deactivation rate constant. Figure 4 shows the plots of DP as a function of reaction time with different water contents in the mixture solvents. We observed that a change in the ratio of methanol to water from 4/1 to 3/2 (v/v) significantly influenced the ATRP process. For a polymerization time of 1 h, solvent with high water content gave a DP that was nearly double that of the lower water content case. This result clearly demonstrated that water acted not only as a diluent but also as an accelerator in the ATRP system. Recently, there

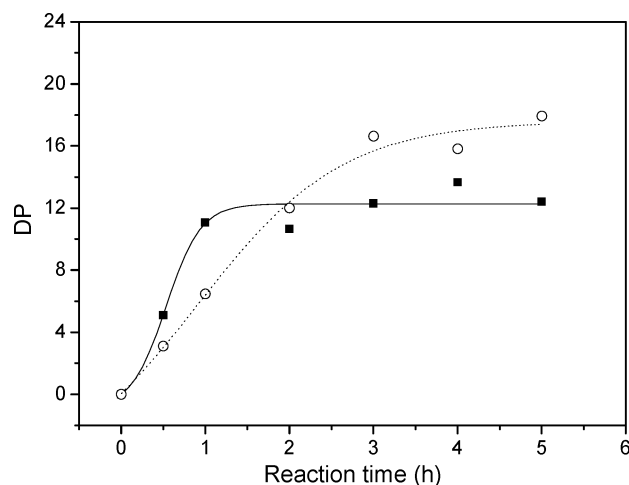


Figure 4. Effect of ATRP time on the DP of grafted PGAMA chains. Surface-initiated ATRP conditions, [GAMA]/[CuBr]/[Bpy] = 100/1/2; solvent, methanol/water = 4/1 (○) and 3/2 (■).

have been several reports on rapid ATRP in the presence of an aqueous medium.^{15h,31,36} For example, poly(glycidyl methacrylate) brushes from a silicon surface were facilitated by a DMF/water solution.^{15h} A PHEMA film of about 700 nm thickness was tethered on the gold surface in an aqueous medium in just 12 h.³¹ The high dielectric constant of the polar solvents, especially water, probably had a marked effect on the structure of the reactants and increased the activity of the catalyst.^{37,38} According to the results of Matyjaszewski,³⁹ in conventional bulk or nonaqueous ATRP, the catalyst systems were neutral, binuclear

(34) (a) Narain, R.; Armes, S. P. *Chem. Commun.* **2002**, 2776. (b) Narain, R.; Armes, S. P. *Biomacromolecules* **2003**, *4*, 1746.

(35) (a) Matyjaszewski, K.; Shipp, D. A.; Wang, J. L.; Grimaud, T.; Patten, T. E. *Macromolecules* **1998**, *31*, 6836. (b) Tsarevsky, N. V.; Pintauer, T.; Matyjaszewski, K. *Macromolecules* **2004**, *37*, 9768.

(36) (a) Wang, X.-S.; Armes, S. P. *Macromolecules* **2000**, *33*, 6640. (b) Robinson, K. L.; Khan, M. A.; Banez, M. V. D.; Wang, X. S.; Armes, S. P. *Macromolecules* **2001**, *34*, 3155. (c) Save, M.; Weaver, J. V. M.; Armes, S. P.; McKenna, P. *Macromolecules* **2002**, *35*, 1152.

(37) Perrier, S.; Haddleton, D. M. *Macromol. Symp.* **2002**, *182*, 261.

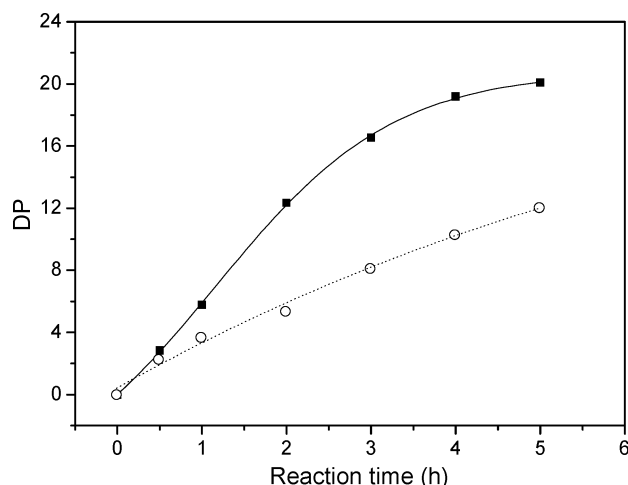


Figure 5. Dependence of PGAMA brush DP on ATRP time with various concentrations of CuBr_2 ($[\text{GAMA}]/[\text{CuBr}]/[\text{CuBr}_2]/[\text{Bpy}] = 100/1/0.25/2$ (■) and $100/1/0.5/2$ (○)); solvent, methanol/water = 4/1.

Cu(I) complexes with bridging halide ligands. However, in aqueous media, the most probable structure of the catalytic species was a monocationic $[\text{Cu(I)}(\text{bpy})_2]^+$ complex with a halide counterion.³² The ionic catalyst species in aqueous media are much more active than the binuclear ones in bulk or nonaqueous systems. The high activity of Cu(I) complexes brings about a high concentration of active species (or radicals) and, subsequently, a high polymerization rate. However, we also found that high water content in the solvent system resulted in a short propagation time and the DP reached plateaus after 1 h, which indicated that the concentration of the propagating species decreased with chain growth. The most reasonable cause of this phenomenon should be the burial of reactive chain ends into the grafted polymer brushes or side reactions such as radical coupling and disproportionation reactions that were promoted in high radical concentration.^{34,40} Table 2 summarizes the ATRP processes under various experimental conditions. The degree of polymerization values in the Table were obtained by two methods. One was the mass weighting method described in the Experimental Section, and the other was based on XPS analysis. For the mass weighting method, we assumed that the initiation efficiency of the immobilized initiator was 100%. However, the efficiency was always much lower. For these reasons, data from mass weighting were lower than those obtained by XPS analysis.

In the ATRP process, the deactivating species is crucial to the equilibrium between the dormant and the active species. To achieve good control over ATRP, a high concentration of deactivating Cu(II) complex is necessary.²⁹ Usually, in bulk ATRP, the Cu(II) species are obtained by the reaction of the Cu(I) complex with the initiator at the beginning of polymerization. However, in surface-initiated ATRP, the relatively low surface initiator concentration prevents the formation of a sufficient amount of the Cu(II) complex to control the polymerization process. Two methods are generally taken to solve this problem. One is the addition of a sacrificial initiator, and the other is the addition of the Cu(II) complex at the beginning of polymerization. Adding sacrificial initiator always results in excessive polymerization of the monomer in solution and often makes the reaction system inhomogeneous. Moreover, ho-

mopolymer in solution often sticks to the substrate surface and interferes with the graft polymerization. In this work, to limit the initiation of polymerization on the surface and to control the concentration of the active species, CuBr_2 was added to the reaction mixture. Figure 5 shows the effect of CuBr_2 on the DP. The monomer/ CuBr ratio and the methanol/water ratio were fixed at 100/1 and 4/1, respectively, whereas a different amount of CuBr_2 was added to the reaction system. With 20 mol % CuBr_2 (relative to CuBr) in the reaction system, the DP increased linearly in the early stage and slowed down after about 3 h. When the CuBr_2 content was increased to 50 mol %, the initial rate of polymerization decreased, but the DP showed a substantial increase over the whole course of the polymerization (6 h). The DP versus time plot also resulted in a linear pattern. In the presence of CuBr_2 , the propagating chain radical was deactivated adequately, and its concentration was low. There was a higher content of CuBr_2 in the ATRP system, and a lower radical concentration was obtained in the polymerization process. Subsequently, a slower polymerization rate was achieved, and on the contrary, the polymerization process was more controllable.

After the surface-initiated ATRP process, the membrane surface was again characterized by FTIR/ATR and XPS. Figure 1d shows the FTIR/ATR spectrum. Compared with that of PPMM-*g*-PHEMA-Br, the spectrum of PPMM-*g*-PHEMA-*co*-PGAMA showed additional peaks at 1659, 1537, and 3510 cm^{-1} that were ascribed to amide I, amide II, and the stretching vibration of the N-H bond, respectively, (Figure 1c,d). In addition, a broad absorption band around 3300 cm^{-1} , assigned to the -OH stretching vibration, was found for PPMM-*g*-PHEMA-*co*-PGAMA. Corresponding variations were also seen for the XPS spectra. The most obvious result of surface-initiated ATRP was the peak appearance of N 1s at 402.8 eV in Figure 2d, which was incorporated by the grafted GAMA chains. The intensity of O 1s peak was even higher than that of the PPMM-*g*-PHEMA-Br surface. This could be ascribed to the grafting of sugar moieties that contain many hydroxyl groups. Moreover, the intensities of the Br 3d (70.5 eV) and Br 3p (187.7 eV) peaks obviously decreased compared to those in PPMM-*g*-PHEMA-Br. This further illuminated the impairment of the living/controlled characterization caused by the loss of terminal C-Br bonds. The high-resolution C 1s peak of the PPMM-*g*-PHEMA-*co*-PGAMA surface was fit with four unique carbon moieties (Figure 3c): C-H (284.7 eV), O=C-NH- (287.7 eV), C-O or C-Br (286.2 eV), and O=C-O (288.4 eV). The additional peak at 287.7 eV was a signal from the C atom in the amide group (O=C-NH-).

Conclusions

Comb-like glycopolymer brushes were successfully tethered onto the PPMM surface by a combination of UV-induced graft polymerization and surface-initiated ATRP. HEMA was first grafted onto the PPMM surface under UV irradiation in the presence of BP and $\text{FeCl}_3 \cdot 6\text{H}_2\text{O}$. The hydroxyl groups on the PHEMA brushes were reacted with 2-bromopropionyl bromide for the coupling of bromide species that subsequently served as the ATRP initiator. Comb-like glycopolymer brushes were then grafted by the surface-initiated ATRP of GAMA. The addition of water to the solvent system increased the polymerization rate significantly; however, it suffered from a loss of controllability. CuBr_2 served as an effective deactivator with which the polymerization process could be well controlled. The chemical changes of the modified membrane surfaces were confirmed by FTIR/ATR and XPS. Further work will focus on the interactions between the surface-tethered glycopolymer and proteins (lectins, albumins, antibodies, and enzymes). With the living/controlled

(38) Haddleton, D. M.; Perrier, S.; Bon, S. A. F. *Macromolecules* **2000**, *33*, 8246.

(39) Kickelbick, G.; Reinohl, U.; Ertel, T. S.; Weber, A.; Bertagnolli, H.; Matyjaszewski, K. *Inorg. Chem.* **2001**, *40*, 6.

(40) Jones, D. M.; Huck, W. T. S. *Adv. Mater.* **2001**, *13*, 1256.

characteristic, one can facilely modulate the interactions by varying the glycopolymer chain length, and there may be prospective applications in affinity surfaces, enzyme immobilization matrixes, and biosensors.

Acknowledgment. Financial support from the National Natural Science Foundation of China (grant no. 20474054), the National Natural Science Foundation of China for Distinguished

Young Scholars (grant no. 50625309), and the Zhejiang Provincial Natural Science Foundation of China (grant no. Z406260) is gratefully acknowledged.

Supporting Information Available: AFM images of the membrane surfaces and the calculation of DP by XPS data. This material is available free of charge via the Internet at <http://pubs.acs.org>.

LA700275T